EARTHQUAKE ENGINEERING AND STRUCTURAL DYNAMICS, VOL. 25, 129–147 (1996)

TESTING OF ENERGY DISSIPATING CLADDING CONNECTIONS

JEAN-PAUL PINELLI
Civil Engineering Program, Florida Institute of Technology, Melbourne, FL 32901-6988, U.S.A.
CHRISTIAN MOOR
Winterthurerstr. 106, 8006 Zürich, Switzerland
JAMES I. CRAIG
School of Aerospace Engineering, Georgia Institute of Technology, Atlanta, GA 30332, USA
AND
BARRY J. GOODNO
School of Civil Engineering, Georgia Institute of Technology, Atlanta, GA 30332, USA

SUMMARY

Properly designed precast concrete cladding could potentially provide lateral stiffness, ductility, and energy dissipation for an overall building structure, especially during earthquakes. This paper describes a set of advanced connections that take advantage of the interaction between facade panels and structure (mainly due to horizontal interstorey drift) to dissipate energy, thereby reducing the response of the main structure. The results of an experimental program to characterize the hysteretic behaviour of advanced connections are presented. Design equations for the advanced connections are then calibrated against the test results, and the corresponding design charts are presented. It is anticipated that this research will lead to innovative ways of viewing the entire cladding system of a building.

KEY WORDS: cladding; connections; energy dissipation; earthquakes

INTRODUCTION

Facades of modern buildings are often clad with architectural heavy precast concrete panels that hang from the structure. They are regarded as a dead weight that does not contribute any structural function to the building. Consequently, structural engineers often leave the choice of cladding and its connections entirely to the architect and precast concrete contractor. Only recently has cladding became a concern to engineers, due to numerous cladding failures, increased competition with other materials for facade enclosures, and renewed interest in methods for passive and active control to attenuate the dynamic response of buildings.

Conventional connection designs[1] try to cancel the interaction between cladding and supporting structure due to seismic-induced interstorey drift by isolating the panel from the main structure. Sliding or flexible connections are recommended to allow movement in the plane of the panel, in this way lessening panel interaction with the supporting frame. However, studies have shown that this disregard of precast panels attached with conventional connections to carry lateral load or add lateral stiffness is not entirely warranted.[2–6] Whether by deliberate design or not, cladding systems (particularly heavy precast systems) can measurably affect the structural stiffness and therefore the dynamic response of buildings. The cladding connections play a critical role in this interaction process.[3]

Instead of minimizing, or cancelling the structure–panel interaction during an earthquake, due mainly to interstorey drift, it is possible to take advantage of it to dissipate energy, thereby reducing the response of the main structure. The key to this new concept of cladding participation is the development of the so-called advanced, or engineered, connections. An advanced connection is one which exhibits superior properties of ductility and damping and results in high energy dissipation without failure during moderate or strong earthquakes. These connections must also limit the forces transmitted into/through the panel. At the same

CCC 0098–8847/96/020129–19

Received 16 February 1994
Revised 15 August 1995

time, the connections must still satisfy the practical criteria of actual conventional architectural connections regarding durability, wind and gravity loads, fabrication, and installation. Last, but not least, the connections must be simple, replaceable, and cost-effective.

Advanced connections must provide both stiffness and damping to the structural system. The stiffness should come into play at low levels of excitation, and guarantee an elastic response for low-intensity earthquakes. The damping, or energy dissipation should be activated at higher level of excitation in the case of moderate or strong seismic motions, and should ensure that inelastic response will be mostly concentrated in the cladding system, thereby sparing the structure from extensive damage.

Analytical studies[8-11] have pointed out that cladding with advanced connections can provide increased stiffness, damping, and ductility to structures subjected to wind and earthquakes because

(a) its position on the periphery of the building, and between floors is ideal for reducing drift, and also torsion;
(b) it offers the opportunity for distributed damping, either spread over the entire facade or in vertical or horizontal bands, as needed to optimize response reductions; and
(c) it is an expensive element that should be fully utilized, and protected, as part of the overall structural system.

There are many different kinds of connection systems for a cladding panel, but they are generally composed of three main components (see Figure 1):

(a) the anchor point, or insert, built into the precast panel provides the panel anchorage;
(b) the connector (often a steel angle), which forms the body of the structural connection between the cladding panel and the main structure; and
(c) the anchor into the building structure (a second insert for a concrete structure or an attachment to a steel member).

Information gained from field studies,[7] insert tests,[12] and analytical modelling of buildings with participating cladding[13] points to the importance of the connector elements in the development of advanced connections. That is where the immediate gains in ductility and energy dissipation can be expected. Tests of inserts alone suggest that by themselves they are not capable of providing the levels of ductility and damping required from an advanced connection without loss of strength and integrity. Furthermore, the codes[14] are adamant in requiring that the ductility be concentrated in the connector body. Therefore, at the present time, research on the development of advanced connections has focused on the connection body (or connector).

This paper is the second in a series of three papers: the first paper[15] describes the test apparatus built to study the advanced connections, and the experimental procedures; this paper is concerned with the identification of advanced connector candidates, their testing, and their design; the third paper[13] deals with the interaction between advanced cladding and structure, and the global design criterion of an advanced cladding system.

ADVANCED CONNECTION CANDIDATES

Several basic concepts have been identified for advanced connections. Ductility and damping can be developed through a number of different passive processes.

Friction mechanism

A friction mechanism is the basis for several actual connection designs proposed by Tyler,[16] Pall,[17] and Palsson.[2] A recent potential candidate for friction-damped cladding connections is the slotted bolted connection developed by Grigorian *et al.*[18]

Large quantities of energy can be dissipated through friction since the inelastic performance is described by rectangular hysteresis loops with negligible fade over several cycles of reversal. However, the reliability of friction-induced mechanisms has yet to be proven. Since there is no slippage during normal operation,

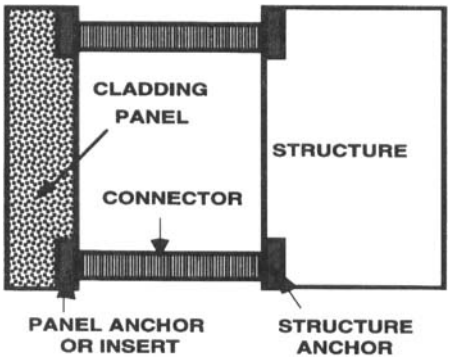

Figure 1. Cladding system

corrosion may increase the friction and change the properties or destroy the mechanism. Also, as in conventional tie-back connections, an insufficient length of the slot could reduce the effectiveness of the friction mechanism.

Composite material mechanism

The connector itself could be a composite system manufactured with different materials selected for strength and ductility, in a manner similar to that in which elastomers are being used in a variety of base isolation systems. Kemeny and Lorant[19] proposed the use of energy dissipating elastomeric cladding connections which had the particularity of providing zero initial stiffness for low levels of excitation.

Plastic deformation mechanism

Many absorbing devices based on the plastification of steel take advantage of the fact that mild steel can reliably provide high stiffness in the elastic range as well as absorb energy with moderate strain hardening when deformed beyond the elastic limit. In addition, steel is relatively easy to manufacture in different shapes, and the stiffness and damping properties of the devices can be improved with judicious choice of geometries. Steel is also economical, and widely used in construction, and therefore it is a material trusted by practitioners.

An attractive plastic deformation mechanism for steel connections is torsion. Torsional devices have some advantages: they have better energy absorption qualities because the uniform distribution of the torsional moment results in a better use of the material, and they exhibit progressive ductile failure distributed over the length of the device.[20] However, the attachment is somewhat complicated if trying to achieve pure torsion in a device between surfaces moving parallel to each other, although the design can be simplified if torsion and bending are combined.

Another promising idea, shown in Figure 2, is inspired by the research reported in Reference 20. In this case, the connector is a ductile closed loop made of mild steel with semi-circular ends. The flexural action in the rolling and unrolling of the loop ends will provide the energy dissipation during a moderate or strong earthquake. The advantage of the loop is its symmetry which makes it suitable for cyclic loading. Also, in a loop, the strain depends on the ratio of thickness to radius and is independent of the displacement.

Advanced connection prototype

Keeping in mind that manufacturing, maintenance, and reliability are as important as a good performance, a series of simple flexural designs for advanced cladding connectors were developed. These are prototypes conceived as a starting point for subsequent more practical implementations. The specimens utilize plastification of steel when stressed beyond yielding in flexure. The same damping mechanism has been investigated in

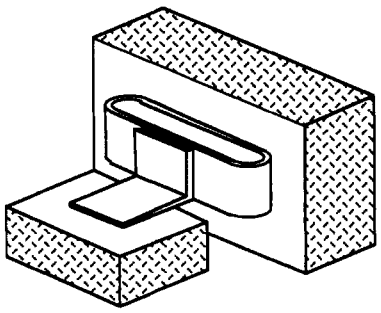

Figure 2. Ductile loop connection

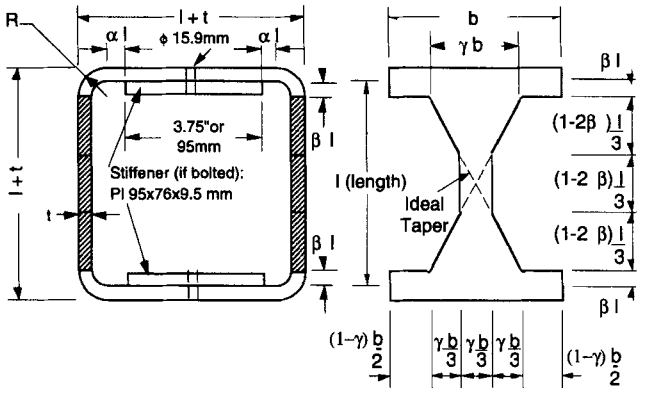

Figure 3. Geometry of tapered connection

the past for foundation supports,[20] and more recently for dampers in piping systems,[21] and for energy dissipating bracing connections.[22]

Details of the design are illustrated in Figure 3. The connector consists of a section of square tube, cut away as shown to create two narrow flexural elements whose widths are tapered to initiate plastification over a greater portion of material. When the tapered elements deform laterally in bending with a double curvature, plastification will occur at all cross-sections along the taper, since both the height of the beam and the bending moment vary linearly. The results will be 'fat', almost rectangular hysteresis loops that reflect the high-energy dissipation resulting from the plastification. In order to get the necessary double curvature (so that the variation in height and moment coincide), it is crucial that the beam's ends be fixed. This fixity is achieved through the cut-away between the supporting untapered elements and the tapered beams, which ensures that the rotational stiffness of the support is higher than the beam's.

The connector could be placed between a panel and the supporting structure through a bolted attachment (where the compression forces are minimized through a vertical slot), as shown in Figure 4. The attachment is composed of two parts: a flexible part, which is the advanced tapered connector itself, and a stiff part which provides a rotational restraint to avoid lateral buckling of the beams of the connector. The still part could be any device. The arrangement proposed here is a square tube welded on top of a steel base plate. The height of the resulting box can be adjusted during installation through a levelling bolt. Once the panel is installed, the box is welded between two steel angles, one on each side. An alternative to the above would be a welded attachment where the tapered tube would be directly welded to the anchor plate and square tube.

The primary objectives of this research were to develop a prototype to proof the feasibility of the advanced connection concept, and to generate sufficient experimental data regarding energy dissipative connections that could be used later in computer simulation of entire building-cladding systems. Complete detailing of

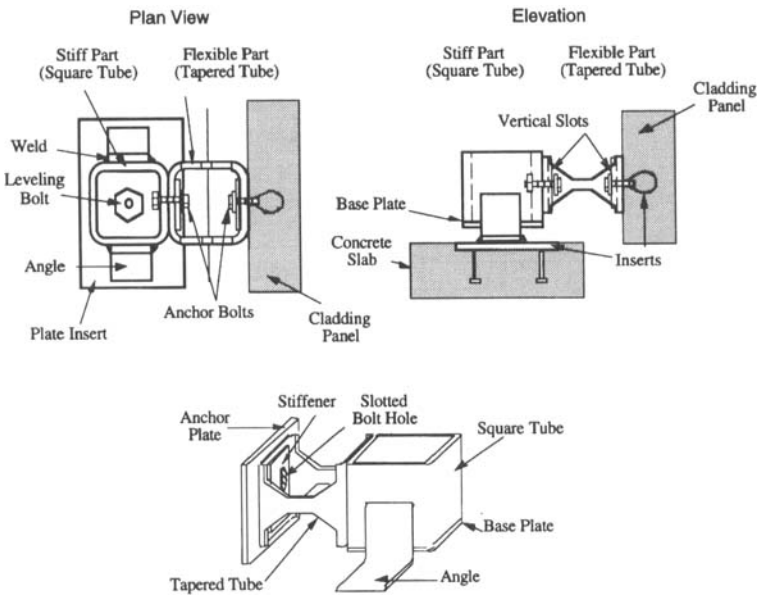

Figure 4. Bolted attachment of advanced connector

Table I. Dimensions of connector specimens (1 in = 25·4 mm)

Specimen name	TT375	TB375, TF375, TW375	TT500	TB250
Tube dimensions	152 × 152 × 9·5 6 × 6 × 0·375	152 × 152 × 9·5 6 × 6 × 0·375	152 × 152 × 12·7 6 × 6 × 0·500	152 × 152 × 6·4* 6 × 6 × 0·250†
Attachment	Welded	Bolted	Welded	Bolted
l (in | mm)	5·625 | 142·9	5·625 | 142·9	5·500 | 139·7	5·750 | 146·1
R (in | mm)	0·75 | 19·1	0·75 | 19·1	1·00 | 25·4	0·50 | 12·7
b (in | mm)	4·50 | 114·3	4·50 | 114·3	4·00 | 101·6	4·50 | 114·3
α	0·044	0·067	0·000	0·109
β	0·100	0·100	0·136	0·065
γ	0·533	0·533	0·525	0·533

* Dimensions in mm
† Dimensions in inches

the connection is certainly the final goal and would be necessary for a practical design, and the proposed attachments can certainly be improved to meet practitioner requirements.

Several tubes with different thicknesses were tested. Figure 3 and Table I give the geometric description of each of them. All the specimens were cut out from 15·2 cm × 15·2 cm (6 in × 6 in) hot rolled square tubes. In all the cases, the central portion of the beams was cut straight to avoid any geometric discontinuity. The material was ASTM A500 grade B steel with a yield stress $\sigma_y = 31{\cdot}7$ kN/cm^2 (46 ksi) in all cases.

Three parameters, α, β and γ, determine the geometry of a tapered connection. They are defined in Figure 3. The variable α represents the portion of the length of the support face of the tube which is straight and not fixed. It is dependent on the type of fixation, and the closer to a situation of total fixity at the flexure ends, the smaller is α. The variable β represents the portion of the length of the beam with full height b (the length itself is computed from centre to centre of opposite faces). The variable γ is the ratio between the

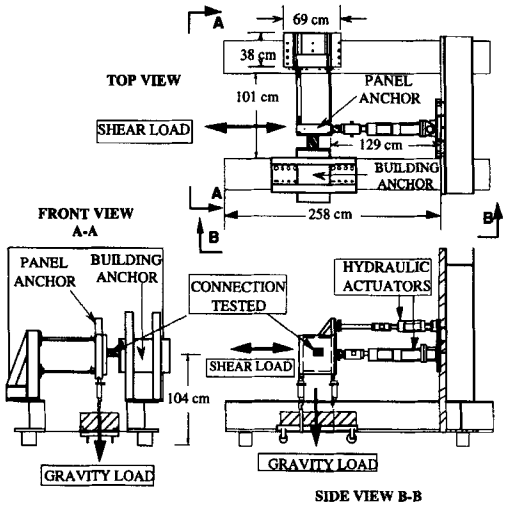

Figure 5. Test fixture for cladding connections

maximum height of the tube and the height of the taper. Both β and γ are dependent on the geometric dimensions and vary with each connector.

TESTING PROGRAM

Testing fixture

A testing machine especially conceived for the study of cladding connections was developed. It is described in detail in Reference 15. The primary objective behind the development of the test apparatus was the simulation of the behaviour of an advanced cladding connection subjected to interstorey drift, and the resulting machine for testing advanced connections had

(a) the ability to isolate and monitor the behaviour of the connector element;
(b) the ability to reproduce the actual service loads and deformations to which a connector is subjected during an earthquake; and
(c) the possibility of testing a variety of damping mechanisms with different conditions of fixity for the connector ends.

Different views of the machine are shown in Figure 5. The fixture is composed of

(a) a rigid steel box (the building anchor) supported on roundway bearings; the box slides back and forth inside two steel frames mounted on a steel I-beam;
(b) a rigidly framed square platform (the panel anchor) facing the steel box; it can move parallel to itself in the horizontal and vertical directions; the platform is linked to a framed rigid support, mounted on another I-beam;
(c) two hydraulic actuators with force capacity of $\pm$ 67 kN (15 kips); the lower and main actuator is a double stroke actuator; it has a stroke of 15·24 cm (6 in), a piston of 33·74 cm^2 (5·23 in^2), and it simulates shear loads or displacements; the upper actuator is a single-stroke actuator that prevents the platform from rotating in its own plane; both are coupled with load cells of up to 89 kN (20 kips) capacity; and
(d) two smaller hand-operated hydraulic actuators that lift the required masses to simulate gravity load in the case of bearing connections; the masses are 24 kg (50 lb) lead blocks stacked on a wheeled cart.

Table II. Summary of advanced connector tests

Specimen ID	Thickness	Attachment	Type of test	Maximum displacement (mm)	Maximum strain (%)	Cycles to failure
TT375	9·5 mm (3/8″)	Welded	Cycles of increasing amplitude to failure	70	10·2	24
TT500	12·7 mm (1/2″)	Welded	Cyc. increasing ampl.	38	9·4	10
			fatigue	31	7·5	16*
TB375	9·5 mm (3/8″)	Bolted	Cyc. increasing ampl.	71	10·2	21
			fatigue	25	3·5	24*
TF375	9·5 mm (3/8″)	Bolted	Fatigue	25	3·5	42
TW375	9·5 mm (3/8″)	Bolted	Fatigue w/increasing gravity load	25	3·5	37
TB250	6·4 mm (1/4″)	Bolted	Cyc. increasing ampl.	74	4·4	20
			fatigue	58	3·5	9*

*Fatigue cycles are in addition to cycles of increasing amplitude

Testing procedure

In the case of an advanced cladding connection, the energy dissipation mechanism is triggered by the interstorey drift during an earthquake, and damping results from a hysteretic process. In view of the relatively small inertia of the connector and the fact that the energy dissipation mechanisms being investigated were assumed to be mainly hysteretic, it was decided that the tests could be quasi-static with the ability to apply cyclic displacements of varying amplitude. Cycles of increasing displacement were applied in small step increments. At each step, displacements and forces were recorded, and the corresponding hysteresis cycles, shear force versus transverse displacement, were plotted. Alternatively, some specimens were tested in fatigue by applying a number of cycles of equal amplitude until the specimens failed.

Tests description

The objective of the tests were

(i) to evaluate the stiffness, ductility and energy dissipation characteristics of each of the connectors;
(ii) to evaluate the influence of different attachment schemes (bolted and welded) on the properties of the connectors;
(iii) to investigate the fatigue behaviour of the connectors; and
(iv) to investigate the influence of a vertical (gravity) load on the lateral behaviour of the connectors.

A series of tests were carried out, involving the specimens presented in Table I. Table II summarizes the characteristics of each of these tests.

TESTS RESULTS

From the force–displacement relationship, several properties regarding forces, stiffnesses, displacement and ductilities were evaluated (see Figure 6 and Table III).

Both conventional and plastic ductilities were quantified. The conventional ductility, μ, is defined as the ratio of the actual displacement to the yield displacement of the first cycle. The equivalent plastic monotonic ductility is the maximum plastic ductility that the system should exhibit in a monotonic loading test in order to dissipate the same amount of energy than during the cyclic loading. The equivalent monotonic plastic ductility demand on the system can be evaluated in terms of energy, and load reversals, as

$$\mu_p = \frac{H_t}{F_y d_y (2N_f)^{0.4}} \tag{1}$$

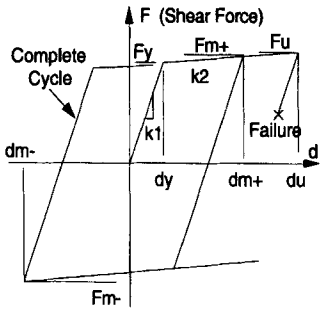

Figure 6. Parameter definitions

Table III. Test results for the tube specimens

Specimen	TT375	TT500	TB375	TB250	Comments (see Figure 6)
k_1 (kN/cm)	36·8	82·3	33·3	8·9	Elastic stiffness
k_2 (kN/cm)	1·4	2·6	1·3	0·5	Postyielding stiffness
k_1/k_2	26	31	25	20	
F_y (kN)	17·8	33·8	16·5	6·2	Yield force
F_u (kN)	29·4	43·2	27·6	11·6	Ultimate force
F_u/F_y	1·65	1·28	1·68	1·86	
F_{m^+} (kN)	27·1	42·3	27·6	10·7	Maximum positive force in a cycle
F_{m^-} (kN)	29·4	43·2	27·1	11·6	Maximum negative force in a cycle
d_y (cm)	0·5	0·4	0·5	0·7	Yield displacement
d_u (cm)	7·0	4·0	7·1	7·4	Ultimate displacement
$\mu = d_u/d_y$	14·4	9·8	14·3	10·6	Conventional ductility
d_{m^+} (cm)	7·0	3·7	7·1	7·4	Maximum positive displacement in a cycle
d_{m^-} (cm)	6·8	4·0	6·7	6·9	Maximum negative displacement in a cycle
H_t (kJ)	35·0	63·6	53·5 49·3*	23·1	Maximum energy dissipated in the test
μ_p	67	72	84 80*	80	Equivalent plastic monotonic ductility

*Values for TF375

where H_t is the total hysteretic energy dissipated in the system during N_f load reversals. This definition of ductility, derived from McCabe and Hall,[23] has the advantage of taking into account the characteristics of the cyclic loading. The corresponding values of μ_p are much higher than those of μ.

TT375 test

The specimen was tested with cycles of increasing displacement amplitude. At the 21st cycle, the test machine maximum permissible displacement was applied, deforming the specimen 70 mm. After three more cycles at the same amplitude, it broke in the middle of the tapered part of one web. The test was continued with one web only and the specimen completely failed shortly thereafter due to the combination of torsion and flexure on the remaining web. The hysteresis loop from the experiment is shown in Figure 7, and the results are presented in Table III.

The hysteresis loop showed an increasing stiffness for displacements above 5·7 cm, which was a consequence of the large deformation. At this level of displacement, the shear force was no longer transmitted by pure bending but by bending and membrane action, which stiffened the device. Because of the increase in stiffness, the ultimate force exceeded the yield force by 65 per cent, but the round corners at the supports still remained elastic and the weld intact. At the extreme displacement of 7·0 cm, the two end plates moved about 2·5 cm closer to each other.

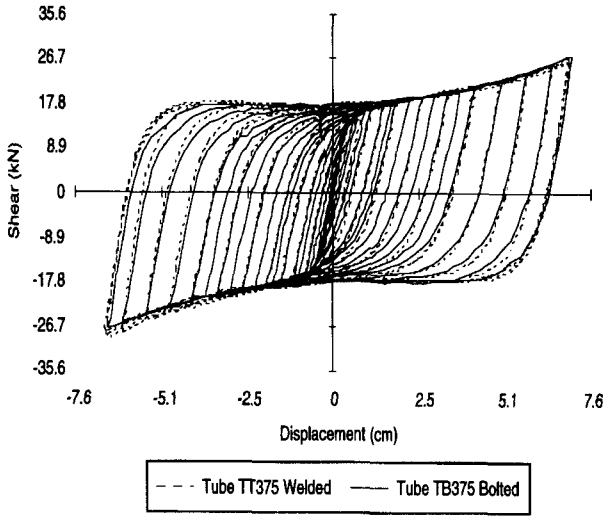

Figure 7. Test results for TB375 and TT375

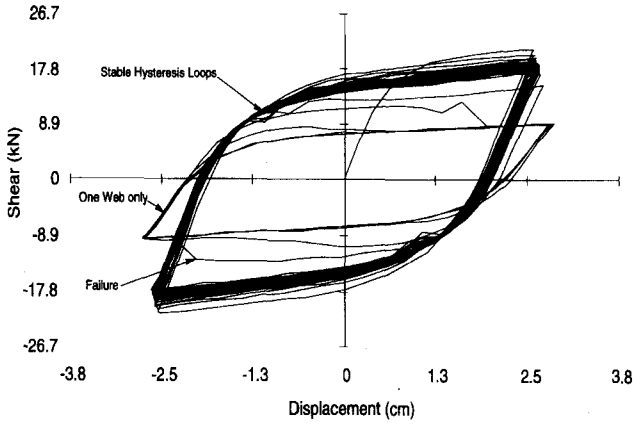

Figure 8. Fatigue test results for specimen TF375

TB375 test

TB375 was attached to the end plates with a single 15·9 mm diameter bolt on each side which replaced the weld of the previous specimen. A 95 × 76 × 9·5 mm washer stiffened the straight faces of the tube (see Figure 3) to ensure the end fixity of the tapered beams.

Three identical specimens were produced and tested in different ways. The first specimen, TB375, was subjected to 21 cycles with increasing amplitude up to 7·1 cm, in a way similar to TT375. No damage was observed during the test. Then the displacement was held constant at 2·5 cm which corresponded to a strain of 3·5 per cent. The specimen failed after an additional 24 cycles due to fatigue. There was no significant difference between TB375 and TT375 (see Figure 7 and Table III).

TF375 test

The second bolted specimen, TF375, was tested for fatigue only (see Tables II and III). The hysteresis loops were stable, showing no stiffness degradation until the first web broke (Figure 8). With only one web, the tube could still provide stiffness and energy dissipation for 9 more cycles, in a very ductile manner.

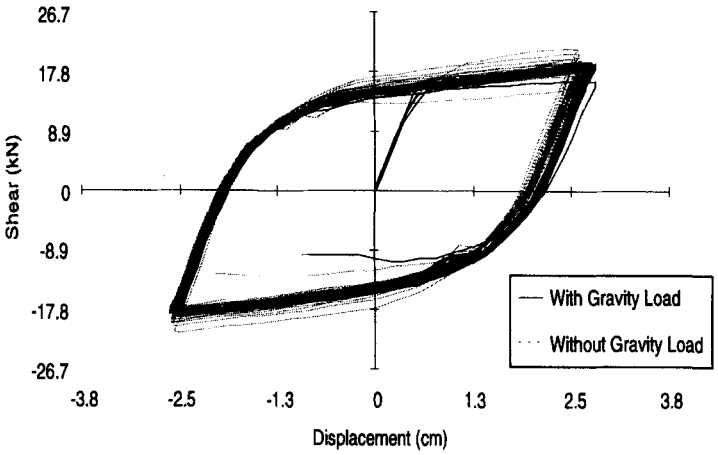

Figure 9. Test results for TF375 (no gravity load) vs. TW375 (gravity load)

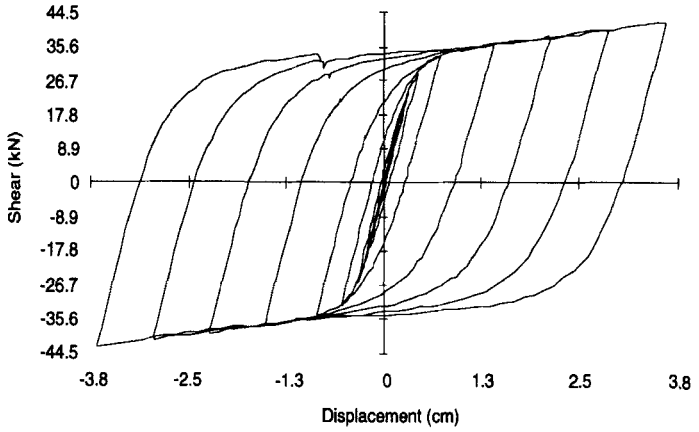

Figure 10. Test results for TT500

TW375 test

The third specimen, TW375, was tested as a bearing connection carrying gravity load in addition to being subjected to the horizontal displacement. The displacement was kept constant at 2·5 cm, and the gravity load was increased with each cycle. After 11 cycles of progressively increasing vertical load, the maximum gravity load of 10·1 kN was added and no cracks were visible. Neither stiffness nor ultimate force was affected by the vertical load and the hysteresis loop was almost the same as that from the test without gravity load (Figure 9), although the total vertical displacement between end plates was 3·0 cm. The specimen was further tested for fatigue with the maximum gravity load of 10·1 kN and 2·5 cm displacement. After 19 additional cycles a crack appeared and the specimen failed after a total of 37 cycles. The hysteresis loops were stable with no stiffness degradation. The gravity load did not affect the lateral behaviour.

TT500 test

A 1·3 cm thick tube was tested to examine the influence of the wall thickness. The specimen was first tested for 10 cycles with increasing amplitude and showed a behaviour similar to the TT375. The results are shown in Figure 10 and Table III. The displacement was limited to 3·8 cm in order to get a maximum strain similar

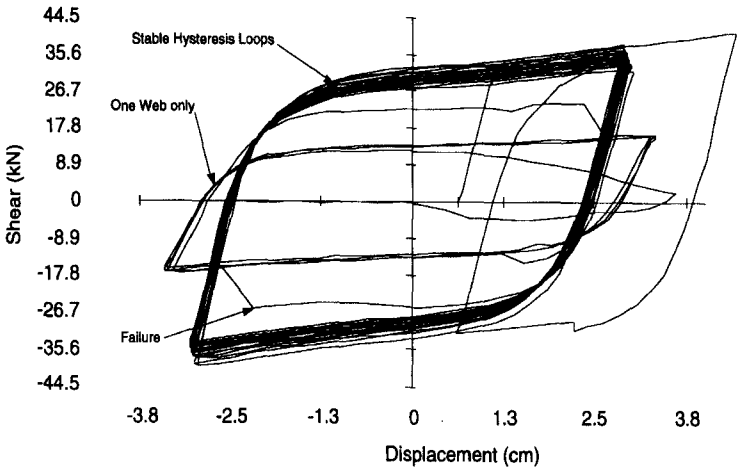

Figure 11. Fatigue test results for specimen TT500

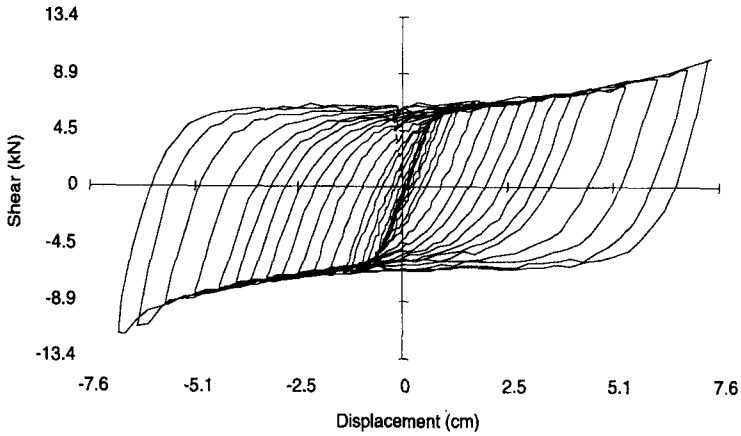

Figure 12. Test results for specimen TB250

to the TT375 case (9·4 per cent strain). A fatigue test was then performed with a displacement of 3·0 cm (7·5 percent strain). The specimen broke after 16 cycles at the transition between the taper and the centre part. The hysteresis loops were stable (Figure 11) with almost no stiffness degradation or strength deterioration.

TT500 showed the same positive characteristics as TT375. The specimen was deformed in double curvature and the attachment zone remained elastic. The weld was also sufficient for the thicker specimen and showed no weakness during the test. The lifetime was low with only 26 cycles, because of the high strain (7·5 vs. 3·5 per cent for TF375) during the fatigue test.

TB250 test

Specimen TB250 was first tested for 20 cycles of increasing amplitude up to a maximum displacement of 7·4 cm (4·4 per cent strain), as shown in Figure 12. A fatigue test was then performed at 3·5 per cent strain (5·8 cm displacement), which lasted 9 cycles until failure (Figure 13). The total lifetime of the specimen was then 29 cycles. This is considerably less than the lifetime of TB375 (45 cycles), which was also identically tested. Apparently, the cracks that occurred in the tapered beams had a shorter way to grow from the surface

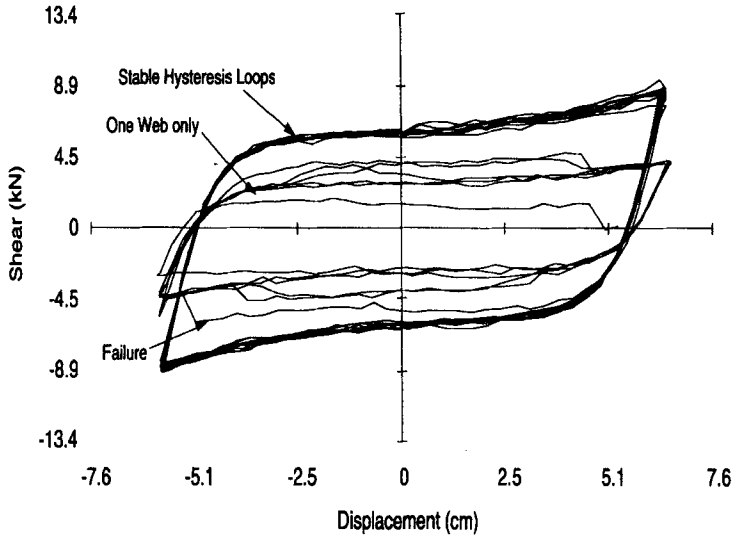

Figure 13. Fatigue test results for specimen TB250

to the centre, reducing the lifetime. The elastic stiffness and the ultimate force were considered to have low values for a cladding connection, which limited its practical use.

Tests conclusions

The tapered advanced connections performed very well in the tests.

(1) In all the cases, the connectors exhibited an advantageous hysteretic behaviour, with fat, stable loops, with no stiffness degradation, or strength deterioration. The plastic deformation was distributed uniformly over the beams, thanks to the taper, resulting in large admissible displacements and a maximum ductility of 14 (see Figures 7 and 12). Higher ductility values could have been obtained since the maximum displacement of the specimens for monotonic failure was beyond the range of the test machine ($\pm$ 7·6 cm). The ductility in this case is defined as the maximum displacement divided by the yield displacement.

(2) The specimens had good low cycle fatigue behaviour, and sustained a large number of cyclic reversals without failure (see Figures 8, 9 and 11). This is in accordance with similar results obtained by Tyler,[24] Bergman and Goel,[25] and Whittaker *et al.*[22] in fatigue tests of tapered steel specimens. For maximum strain not exceeding 3·5 per cent the maximum number of cycles was close to 40. In an actual building, the allowable storey drift should result in even lower strains, and hence longer lifetime. In almost all cases, the fracture occurred at the transition between the taper and the centre straight part, probably due to stress concentrations at the kick in the steel shape. This suggests that a more elaborate manufacturing with round corners at the transition zones will translate in a higher number of cycles before failure.

(3) Whether the specimen is bolted or welded has no influence on its behaviour (see Figure 7). The fact that the connector can be bolted to the insert with a single bolt (like many conventional connectors), without any drawback in performance, makes it very attractive from an installation and maintenance point of view.

(4) In previous test reports on tapered specimens,[24,22] the key issue has always been the provision of a sufficiently fixed condition for the ends of the tapered beams. The design presented here provides a simple and effective solution through the use of a reduced width of the flexural elements.

(5) The failure of each tapered specimen was shown to be very ductile. The failure always initiated in one of the two tapered beams through some progressive cracking. After failure of one beam, the remaining

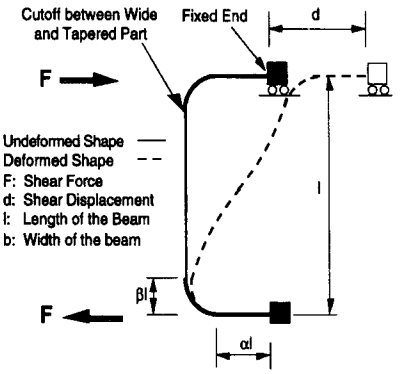

Figure 14. Two-dimensional beam model for the tube specimens

beam provided an additional reserve of strength and ductility for a few extra cycles (see Figures 8, 9, 11 and 13).

(6) The specimen can sustain vertical loads without losing its energy dissipation capabilities (see Figure 9). This result indicates that the specimen should be able to perform adequately in the presence of combined high vertical and horizontal accelerations like the ones observed in the 1994 Northridge earthquake, although the presence of a vertical slot in the bolted connection (see Figure 4) should minimize the influence of the vertical loading. More testing involving cyclic loading in both directions should be done to verify this point. The result also shows that some of these tapered designs could be used for combined bearing and energy dissipating connections.

This last point requires some additional comments. On the basis of safety concerns,one could question the merit of combining gravity load support with energy dissipation. However, if it can be proved through adequate testing that an energy dissipator can provide both, then the possibility should not be discarded. Although the use of bearing energy dissipators is not advocated here, the key point is the fact that vertical loads do not necessarily adversely affect the lateral behaviour and energy dissipation of the tapered connector.

DESIGN CONSIDERATIONS

The two-dimensional beam model shown in Figure 14 (the figure shows only one of the two symmetric tapered beams) was adopted for preliminary analytical computations of the elastic stiffness and the yield force of each specimen. The curved parts account for the rounded corners of the tube and the length is measured between the centreline of two opposite faces. The width of the taper varies along the beam according to Figure 3, and the thickness is constant. The force required to reach plastification is called the yield force, and the corresponding displacement the yield displacement.

It can be shown that if $\gamma/(1-2\beta) < 1$, then the plastification starts in the taper for a value of yield load

$$F_y = \frac{\sigma_y b t^2}{l} \frac{\gamma}{1-2\beta} \tag{2}$$

The corresponding yield displacement of two curved beams as in Figure 14 is equal to

$$d_y = F_y \frac{l^3}{2\,Eb\,t^3} \eta \tag{3}$$

Table IV. Values of η for tapered tubes

Specimen	From equation (4)	From tests	Design value
TB250	3·1	4·2	4·0
TB375	2·7	4·1	4·0
TT500	2·2	3·7	4·0

with the correction factor

$$\eta = \left(\frac{3}{2\gamma} + 6\alpha\right) + \left(-\frac{9}{\gamma} + 9{\cdot}4248\right)\beta + \left(\frac{18}{\gamma} - 13{\cdot}2992\right)\beta^2 + \left(-\frac{12}{\gamma} + 8{\cdot}5488\right)\beta^3 \tag{4}$$

α, β, and γ are defined in Figure 3, and vary with each specimen (see Table I).

The resulting elastic stiffness is equal to

$$k_1 = \frac{F_y}{d_y} = \frac{2\,Eb\,t^3}{l^3\,\eta} \tag{5}$$

Equations (2) and (5) are valid as long as the necessary conditions of fixity are provided at both ends of the connector. It was shown previously that fixity can be achieved through a welded or a bolted attachment. In both cases the anchor plate or device to which the connector is attached has to be rotationally fixed to the structure or panel if lateral buckling of the beams of the connector is to be avoided. For the bolted connections, it is estimated that the washer distributes the fixation over the washer area. In the case of welded attachment, where the connectors are only welded along their lower and upper edges, the finite transverse bending stiffness reduces the end fixity. The wider is the specimen, the less appropriate is the beam model. In addition, the fixation in the machine is never perfectly rigid. But the model was nevertheless considered accurate enough to give a preliminary estimate of strength and stiffness.

The values of elastic stiffness, yield force and yield displacement computed according to equations (2)–(5) are compared in Table V to the test results. The much lower experimental stiffness can be explained by the lack of perfect rotational restraint at the ends of the tapered beams, which is more important in the case of welded attachments. Another fundamental source of error, responsible for the higher experimental yield force, is the difference between nominal and actual values for the material properties of steel such as the elastic modulus and, more importantly, the yield stress σ_y. For this reason, it is recommended that actual values computed from laboratory tests be used whenever possible for the material properties. It is also difficult to define an exact yield force from the tests since there is no well-defined yield point, and the specimens smoothly change from the elastic to the inelastic behaviour by a continuous decrease of stiffness.

In view of the discrepancies between analytical and experimental values, the analytical expressions (2) and (5) were transformed in design equations, as follows:

(a) new values of the correction factor η were computed to match the test results; they are given for each specimen in Table IV, from which an average design value of $\eta_d = 4{\cdot}0$ was adopted;
(b) the width reduction, as defined by γ, was judged adequate, since the attachment zone remained elastic in all tests; to standardize all connections, a value of $\gamma_d = 0{\cdot}5$ was chosen;
(c) since the value of β is unknown at the beginning of a design, a standard value of $\beta_d = 0{\cdot}115$ was adopted for the design equation; and,
(d) finally, in the absence of actual data on the real values of the steel yield stress, the nominal values specified by the manufacturer must be used in the design equations.

Table V. Comparison of preliminary calculations with test results

Specimen	Property	Analytical	Tests	Ratio	Design
Tube 500	k_1 (kN/cm)	141·9	82·3	0·6	80·6
Welded	F_y (kN)	26·7	33·8	1·3	24·0
(TT500)	d_y (cm)	0·2	0·4	2·3	0·3
Tube 375	k_1 (kN/cm)	54·3	36·8	0·7	33·8
Welded	F_y (kN)	15·6	17·8	1·1	15·1
(TT375)	d_y (cm)	0·3	0·5	1·7	0·4
Tube 375 bolted	k_1 (kN/cm)	42·9	33·3	0·8	33·8
(TB375, TF375,	F_y (kN)	15·6	16·5	1·1	15·1
TW375)	d_y (cm)	0·4	0·5	1·4	0·4
Tube 250 bolted	k_1 (kN/cm)	12·8	8·9	0·7	9·5
(TB250)	F_y (kN)	6·2	6·2	1·0	6·7
	d_y (cm)	0·5	0·7	1·42	0·7

The resulting value of $\gamma/(1-2\beta) = 0{\cdot}65$ compares well with the actual values of 0·61, 0·67, and 0·72 for the specimens TB250, TB375, and TT500, respectively. The resulting design equations are

$$k_1 = \frac{2\,Ebt^3}{l^3\,\eta_d} = \frac{Ebt^3}{2l^3} \tag{6}$$

$$F_y = \frac{\sigma_y b t^2}{1}\,\frac{\gamma_d}{1-2\beta_d} = \frac{\sigma_y b t^2}{1}0{\cdot}65 \tag{7}$$

The last column of Table V lists the values of k_1, F_y, and d_y computed with equations (6) and (7) for each of the specimens.

Based on equations (6) and (7) it is possible to check that these so-called advanced or engineered connectors do satisfy the minimum requirements for strength specified in the code.[14] For example, for a 10·7 kN cladding panel, the force to be resisted by the connector body should be, according to the code,

$$F = 1{\cdot}33\,ZIC_p\,W_p = 1{\cdot}33 \times 0{\cdot}4 \times 1 \times 0{\cdot}75\,W_p = 0{\cdot}4W_p = 4{\cdot}3\text{ kN} \tag{8}$$

From equation (7), any tapered connector with a height b of 9·1 cm, a length l of 15·2 cm, and a thickness equal to or greater than 0·6 cm will satisfy the above strength requirements.

DESIGN EXAMPLE

In order to test the validity of the proposed advanced cladding connection system, analytical models of the connection elements were developed and calibrated against the experimental results. They were then incorporated into a two-dimensional structural model of a six-storey, two bay building that carries two heavy cladding panels per bay as shown in Figure 15. All the panels on the facades of the building are attached with two bottom conventional bearing connections, and two top advanced tapered tie-back connections of the type described above (but with $\sigma_y = 24{\cdot}8$ kN/cm^2 = 36 ksi). A detailed description of the framed structure, and the corresponding analytical studies of the interaction between cladding and structure, can be found in References 10 and 13.

The cladded structure was subjected to several different ground motions, with different frequency content. In each case, the optimal connector design was identified as being the one that provided the highest ratio of energy dissipated in all the connection over the relative energy input to the structure by the earthquake. At the same time, the connections had to satisfy the necessary ductility requirements, the code strength requirements, and the forces induced into the panels were limited to 44·5 kN (10 kips).

For each earthquake, it was shown that the tapered connections dissipated enough energy to keep the response of the structure successfully into the linear elastic range, with the corresponding reductions in drift

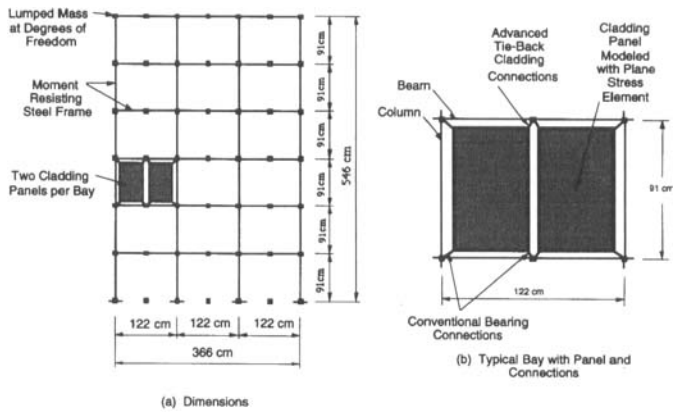

Figure 15. Frame with cladding panels and advanced cladding connections

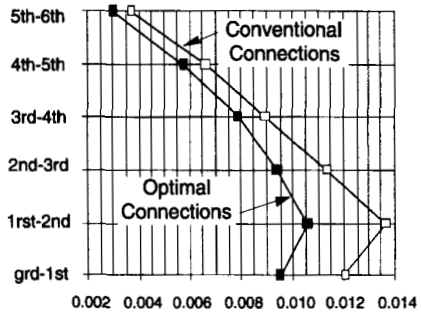

Figure 16. Drifts envelopes—Chile

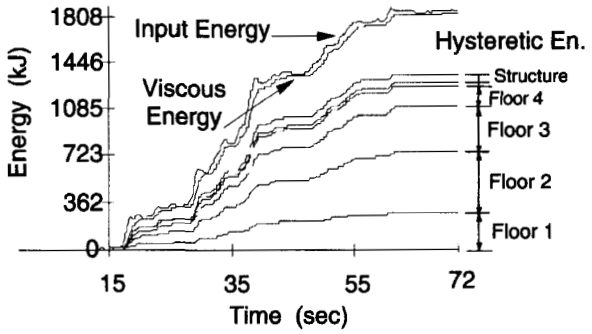

Figure 17. Energy time history—Chile

and displacements. Figure 16 shows the reduction in interstorey drifts (expressed as a fraction of storey height) due to advanced cladding when the structure was subjected to the S20W Viña del Mar record of the Chile earthquake of 1985 (maximum acceleration 0·36 g, duration 100 sec). It was found in this case that the optimal values of stiffness k_1 and yield load F_y for the tapered connector are 27·3 kN/cm (15·6 kips/in), and 11·4 kN (2·56 kips), respectively.

Figure 17 shows how the energy is dissipated in the connections at the different floors for the entire duration of the earthquake. It can be seen that the connections are highly successful at dissipating

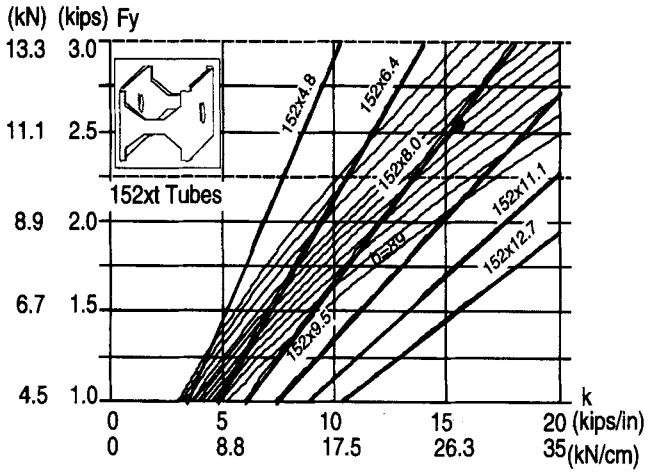

Figure 18. Design chart for 152 mm (6 in) long tapered connectors

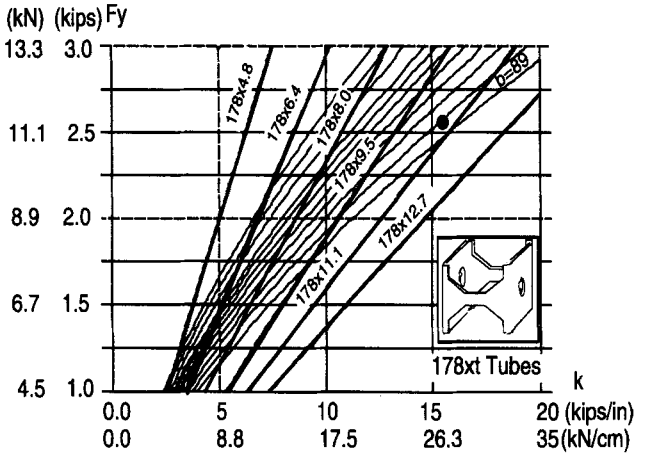

Figure 19. Design chart for 178 mm (7 in) long tapered connectors

a substantial amount of the input energy, but that this dissipation occurs mainly in the first four floors, where the maximum drifts occur. The contribution of the connections of the last two floors is almost non-existent due to the small interstorey drift between the upper floors. Consequently, if it were necessary to dissipate more energy, connections with different properties could be located at different heights on the facade. The figure also shows that during the first 17 sec of the of the earthquake, the connections dissipate almost no energy due to the low level of the excitation. At this early stage, the connections remain elastic and contribute to the response by increasing the lateral stiffness of the structure.

The design equations (6) and (7) can be combined, and represented graphically in design charts like the ones shows in Figures 18 and 19, for 152 mm (6 in) long tapered tubes, and 178 mm (7 in) long tapered tubes. For each length of tube, the straight lines correspond to the different thicknesses t, available in the marketplace, and the curved lines correspond to different heights b, starting at $b = 89$ mm (3·5 in) (lowest line) with successive increments of 13 mm (0·5 in). Once the optimal values of yield load and stiffness for a connector have been obtained through analysis, the geometric dimensions of the device are readily

available from the charts. For example, the optimal values of k and F_y in the case of the Chilean earthquake can translate into a 152 × 152 × 8 mm (6″ × 6″ × 0·313″) tapered tube with a height b = 16·5 cm (6·5″), or into a 178 × 178 × 11 mm (7″ × 7″ × 0·438″) tapered tube with a height b = 9·1 cm (3·6″).

CONCLUSIONS

Advanced cladding connections can be conceived using several different energy dissipation mechanisms. A prototype for an advanced connection has been presented here that takes advantage of plastification of steel when in flexure. The connection is simple, easy and economical to manufacture, and it can be installed through a simple bolted attachment. Laboratory tests have demonstrated that it satisfies the necessary requirements of ductility, strength, dissipation, and repeatability in its hysteretic behaviour, and that it responds adequately to low cycle fatigue phenomena.

When installed on a framed structure in a computer simulation, the advanced cladding has been shown to protect the structure from incurring inelastic behaviour, and to reduce the seismic response. The necessary values of stiffness and yield load for the advanced connections can be readily translated in actual geometric dimensions with the help of the design charts for tapered advanced connections presented here.

These design charts have been developed on the basis of a small series of tests, on a small number of prototype connections. Further testing involving more devices, and a greater number of tests should be carried out in order to be able to generalize truly the results presented here. However, the present studies do demonstrate the great potential of advanced cladding as an alternative choice for passive control systems for seismic design of new structures, or for retrofit of existing buildings.

ACKNOWLEDGEMENT

The support of the National Science Foundation, through Grant BCS-8906508 is gratefully acknowledged. However, the findings and opinions expressed here are those of the authors and do not represent the position of the NSF.

REFERENCES

1. PCI, 'Manual on design and typical details of connections for precast and prestressed concrete', 2nd edn., PCI, Chicago, IL, 1988.
2. H. Palsson, B. Goodno, J. Craig and K. Will, 'Cladding influence on dynamic response of tall buildings', *Earthquake eng. struct. dyn.* **12**, 215–228 (1984).
3. M. L. Wang, 'Cladding performance on a full scale test frame', *Earthquake spectra*, **3**, 119–173 (1987).
4. S. S. Rihal, 'Seismic behavior and design of precast facades, cladding and connections in low/medium-rise buildings', *Report ARCE R88-1*, California Institute of Technology, 1988.
5. R. Gaiotti and B. S. Smith, 'Stiffening of moment-resisting frame by precast concrete cladding', *PCI j.* **37**, 80–92 (1992).
6. R. L. Sack, R. J. Beers and D. L. Thomas, 'Seismic behavior of architectural precast concrete cladding', *Proc. int. symp. on architectural precast concrete cladding*, Chicago, IL, 1989, pp. 141–158.
7. B. Goodno, J. Craig, L. El-Gazairly and C.-C. Hsu 'Use of advanced cladding systems for passive control of building response in earthquakes', *Proc 10th WCEE*, Madrid, Vol. 7, 1992, pp. 4183–4188.
8. B. Goodno and H. Palsson, 'Analytical studies of building cladding', *J. struct. eng. ASCE*, **112**, 665–676 (1986).
9. R. M. Henry and F. Roll, 'Cladding-frame interaction', *J. struct. eng. ASCE* **112**, 815–834 (1986).
10. J. -P. Pinelli, J. I. Craig, B. J. Goodno and C. C. Hsu, 'Passive control of building response using energy dissipating cladding connections', *Earthquake spectra*, **9**, 529–546 (1993).
11. J. M. Cohen and G. H. Powell, 'A design study of an energy dissipating cladding system', *Earthquake eng. struct. dyn.* **22**, 617–632, (1993).
12. J. -P. Pinelli, J. I. Craig, B. J. Goodno, 'Development and calibration of selected dynamic models for precast cladding connections', *Proc. 4th USNCEE*, vol. 2, 1990, pp. 147–156.
13. J. -P. Pinelli, J. I. Craig and B. J. Goodno, 'Energy-based seismic design of ductile cladding systems', *J. struct. eng. ASCE*, **121**, 567–578 (1995).
14. Uniform Building Code, International Conf. of Bldgs Officials, 5360 S. Workman Mill Rd., Whittier, CA, 90602, 1991.
15. J. -P. Pinelli, C. Moor, J. I. Craig and B. J. Goodno, 'Experimental testing of ductile cladding connections for building facades', *Struct. des. tall buildings*, 57–72 (1992).
16. R. G. Tyler, 'Damping in building structures by means of PTFE sliding joints', *Bull. New Zealand soc. earthquake eng.* **10**, (1977).
17. A. S. Pall, 'Friction damped connections for precast concrete cladding', *Proc. int. symp. on architectural precast concrete cladding*, Chicago, IL, 1989, pp. 300–310.

18. C. E. Grigorian, T. S. Yang and E. P. Popov, 'Slotted bolted connection energy dissipators', *Earthquake spectra* **9**, 491–504 (1993).
19. Z. Kemeny, and J. Lorant, 'Energy dissipating elastomeric connections', *Proc. int. symp. on architectural precast concrete cladding*, Chicago, IL, 1989, pp. 287–299.
20. J. M. Kelly, R. I. Skinner and A. J. Heine, 'Mechanisms of energy absorption in special devices for use in earthquake resistant structures', *Bull. New Zealand soc. earthquake eng.* **5**(3), 63–88 (1972).
21. S. Schneider, H. M. Lee and W. Godden, 'Piping seismic test with energy-absorbing devices', *Final Report, EPRI-NP-2902*, Research Project 1586-1, EERC, U. C. Berkeley, CA, March 1983.
22. A. S. Whittaker, V. Bertero, C. Thompson and L. Alonso, 'Seismic testing of steel plate energy dissipation devices', *Earthquake spectra* **7**, 563–604 (1991).
23. S. L. McCabe and W. J. Hall, 'Assessment of seismic structural damage', *J. struct. eng. ASCE* **115**, 2166–2183 (1989).
24. R. G. Tyler, 'Tapered-steel energy dissipators for earthquake resistant structures', *Bull. New Zealand soc. earthquake eng.* **11**, 282–294 (1978).
25. D. M. Bergman and S. C. Goel, 'Evaluation of cyclic testing of steel-plate devices for added damping and stiffness', *Report No. UCME 87-10*, Department of Civil Engineering, University of Michigan, Ann Arbor, MI, November 1987.